# COCHLEAR IMPLANT ARTIFACT REJECTION IN ELECTRICALLY EVOKED AUDITORY STEADY STATE RESPONSES

*Hanne Deprez*[1 2]*, Michael Hofmann*[2]*, Astrid van Wieringen*[2]*, Jan Wouters*[2] *and Marc Moonen*[1]

[1]STADIUS, Dept. of Electrical Engineering (ESAT), KU Leuven
Kasteelpark Arenberg 10, 3001 Leuven, Belgium
[2]ExpORL, Dept. of Neurosciences, KU Leuven
Herestraat 49 bus 721, 3000 Leuven, Belgium

## ABSTRACT

Electrically evoked auditory steady state responses (EASSRs) are EEG signals measured in response to periodic or modulated pulse trains presented through a cochlear implant (CI). EASSRs are studied for the objective fitting of CIs in infants, as electrophysiological thresholds determined with EASSRs correlate well with behavioural thresholds. Currently available techniques to remove CI artifacts from such measurements are only able to deal with artifacts for low-rate pulse trains or modulated pulse trains presented in bipolar mode, which are not used in main clinical practice. In this paper, an automatic EASSR CI artifact rejection technique based on independent component analysis (ICA) is presented that is suitable for clinical parameters. Artifactual independent components are selected based on the spectral amplitude of the pulse rate. Electrophysiological thresholds determined based on ICA compensated signals are equal to those detected using blanked signals, but measurements at only one modulation frequency are required.

***Index Terms***— CI artifact, EASSR, objective, automatic, ICA

## 1. INTRODUCTION

In profoundly deaf or severely hearing impaired subjects, a cochlear implant (CI) can restore hearing. The auditory nerve is electrically stimulated through an electrode array implanted into the cochlea. An increasing number of infants are implanted with a CI, as early implantation has been proven to be crucial for speech and language development [1]. For a CI, the electrodes of the array have to be fitted to the individual characteristics of the electrode-nerve interface. Minimal and maximal comfortable stimulation levels (T and C levels, respectively) for each stimulation electrode are adjusted to the dynamic range of the CI recipient based on behavioural responses from the subject. For infants, behavioural fitting is challenging, as the subjects cannot give verbal feedback about the perceived loudness of the stimuli.

Several techniques for the objective fitting of CIs based on electroencephalogram (EEG) measurements have been evaluated. Transient responses measured at the neuron-electrode interface (electrically evoked compound action potentials or ECAPs) and at the brainstem level (electrically evoked auditory brainstem responses or EABRs) have been considered but are not capable of reliably predicting the behavioural thresholds [2, 3].

Recently, it has been shown that electrically evoked steady state responses (EASSRs) result in electrophysiological thresholds that correlate well with behavioural T levels at clinical pulse rates in bipolar mode [4, 5]. EASSRs can be measured from the auditory system in response to the envelope of periodic or modulated pulse trains [6]. They are objectively detected in the EEG spectrum at the modulation frequency of the pulse trains based on a statistical test, e. g. an F-test or a Hotelling $T^2$ test [7] [8].

As EASSRs are recorded in response to electrical stimulation, measurements are corrupted by artifacts caused by the electrical stimulation pulses and by the radio frequency (RF) transmission link between the external speech processor and the internal implant. These artifacts contain a component at the modulation frequency [9] and must therefore be removed prior to response detection.

For brain responses based on transient stimuli such as ECAPs, EABRs and cortical auditory evoked responses (CAEPs), several CI artifact rejection techniques have been considered. For artifacts and neural responses that do not overlap in frequency, simple frequency domain filtering may be appropriate. Some studies have used short duration stimuli such that the CI artifact and the response do not overlap in time [10, 11]. Artifacts can also be attenuated with a subtraction technique, in which the experimental conditions are

This research work was carried out at the ESAT Laboratory of KU Leuven and at ExpORL, Dept. Neurosciences of KU Leuven, in the frame of Research Project FWO nr. G.066213 'Objective mapping of cochlear implants', IWT Project 'Signal processing and automatic fitting for next generation cochlear implants', KU Leuven Research Council CoE PFV/10/002 (OPTEC) and Concerted Research Action GOA-MaNet. The scientific responsibility is assumed by its authors

varied such that the responses change, while the CI artifact remains constant and can be subtracted [12]. Re-referencing and optimal differential recording electrode configurations are effective, but a large inter-subject variability exists, and determining the optimal recording electrode combination is cumbersome [10, 11]. Beamforming based CI artifact rejection has been investigated in [13]. For transient responses such as CAEPs, CI artifact rejection based on independent component analysis (ICA) has been investigated [10, 11, 14]. Here, the challenge is to determine which independent components (ICs) belong to the CI artifact, as manual IC selection is time consuming and subjective. In [15], a semi-automatic CI artifact IC selection technique has been developed.

Despite the abundance of CI artifact rejection techniques for transient responses, specialized techniques for steady-state responses such as EASSRs have not yet been studied intensively. Usually, stimuli of alternating polarities are presented and the averaging of sweeps of both polarities results in a signal where the CI artifact is attenuated, while the response remains unchanged [4–6, 10, 11]. The remaining CI artifact is then removed based on interpolation over the duration of the CI artifact [4, 5]. Especially for monopolar mode, where stimulation is between an internal stimulation electrode and a stimulation electrode outside the cochlea, this technique fails to remove the entire CI artifact. For response detection, it must be combined with a two-sample statistical test which is robust in the presence of CI artifacts. However, because measurements at two modulation frequencies are needed, the measurement time is doubled. Furthermore, response properties such as amplitudes and apparent latencies cannot reliably be investigated in the presence of residual CI artifact.

In this paper, an automatic EASSR CI artifact rejection technique based on ICA is presented and compared to other EASSR CI artifact rejection techniques currently in use. Results of a pilot experiment in one CI subject are presented and discussed.

## 2. MATERIALS AND METHODS

### 2.1. Blanking and a two-sample statistical test for response detection

Blanking is the state of the art method for EASSR CI artifact rejection [4]. The CI artifact is strictly time-locked to the stimulus pulses. When a CI artifact occurs, the signal is replaced by the first order polynomial interpolation over the CI artifact duration. Stimulation mode has an influence on the CI artifact characteristics: monopolar stimulation mode results in a longer and larger CI artifact than stimulation in bipolar mode. For measurements in monopolar mode, blanking is usually combined with a statistical response detection method such as a two-sample Hotelling $T^2$ test that is robust in the presence of a residual CI artifact. The test distinguishes between CI artifact and response by evaluating both at two modulation frequencies, hence doubling the measurement time.

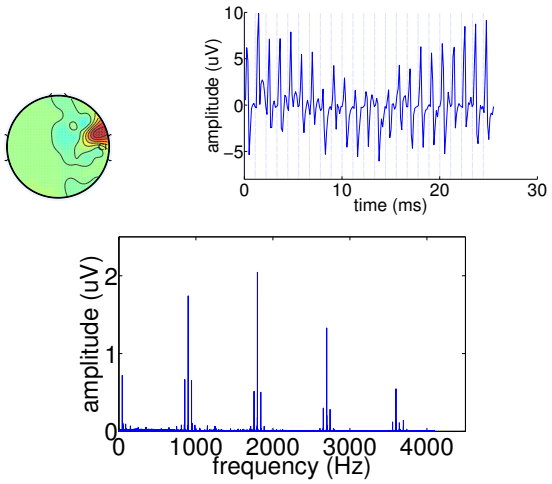


**Fig. 1**. Space (top row, left), time (top row, right) and frequency (bottom row) domain representation of the CI artifact, approximated as the averaged difference between non-blanked and blanked signals. In the top row, right, the pulse period is indicated with vertical dotted lines. Recording electrode $TP_8$, stimulation electrodes 10 and 5, AM pulse train presented in bipolar mode between 0 and 200 cu, $f_{\text{mod}} = 44$ Hz, $f_{\text{pulse}} = 900$ Hz, phase width 40 µs, phase gap 8 µs.

### 2.2. CI artifact characterisation

To characterize the CI artifact, non-blanked and blanked signals were subtracted and averaged (figure 1). EASSRs in response to bipolar presented pulse trains were used, as blanking is effective in rejecting CI artifacts for bipolar stimulation mode. The pulses were amplitude modulated (AM) with a frequency of 44 Hz and a pulse rate of 900 pulses per second (pps) and presented between two internal stimulation electrodes. The CI artifact was time-locked to the stimulus and localized close to the RF coil. It exhibited the typical spectrum of an AM pulse train, with main frequency components at the pulse rate and its side bands and at the modulation frequency. The contribution of the artifact at the modulation frequency heavily depends on the CI artifact asymmetry.

### 2.3. ICA and selection of CI artifact independent components

ICA separates a multichannel signal into statistically maximally independent components (ICs). The multichannel signal is first decorrelated using principal component analysis (PCA). Next, the mixing matrix is iteratively adjusted, to result in maximally independent components.

To isolate the response, ICs associated with the CI artifact

have to be identified and removed. In a first stage, the ICs were selected manually based on their (1) frequency domain representations and (2) spatial signatures. For the frequency domain, ICs that contained energy peaks at the pulse rate and its side bands were selected as artifactual ICs. Similarly, in the spatial domain, ICs that were mainly located around the RF coil were selected as artifactual ICs.

In a second phase, CI artifact IC selection was automated by thresholding. We assume that the typical properties of AM pulse trains are reflected in the ICs (i. e., the ratio between the pulse rate component and the side bands at $f_{\text{pulse}} \pm f_{\text{mod}}$ is fixed and depends on the modulation depth). Furthermore, we assume that the CI artifact is asymmetric and contributes maximally to the modulation frequency (i. e., the side band amplitudes are equal to the modulation frequency amplitude). For each IC, the maximum value for the pulse rate spectral amplitude was determined, such that the maximal artifactual contribution of this IC to any electrode at the modulation frequency never exceeds the noise level of approximately $50$ nV. All ICs for which the pulse rate spectral amplitude exceeded this predefined threshold value, were selected as artifactual ICs.

After artifact IC selection, the artifactual ICs were subtracted from the measured signals, leading to CI artifact compensated measurements. Figure 2 shows the time and frequency domain distributions of the uncompensated and compensated responses, as well as of the estimated artifact. The uncompensated response is dominated by the artifact, with a big pulse rate amplitude component. Residual CI artifact is present in the ICA-compensated response, but is not dominant anymore. The amplitude of the pulse component is reduced by almost a factor $50$. The estimated CI artifact exibits the same properties as the CI artifact obtained by blanking for measurements in bipolar mode: the artifact is time-locked to the stimulus pulse rate and has a dominant spectral pulse rate component.

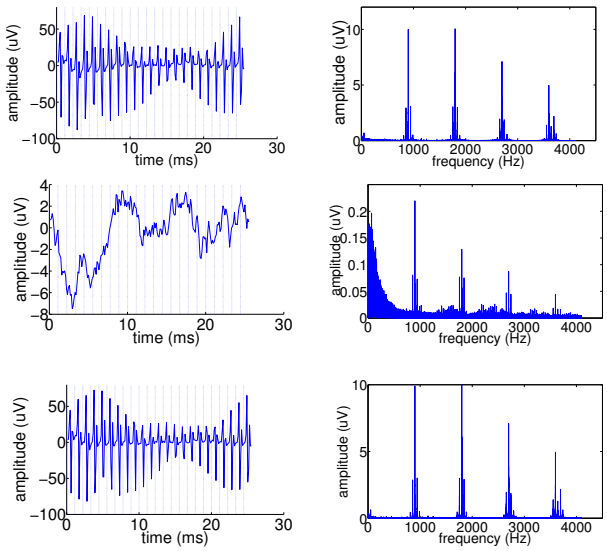


**Fig. 2**. Time and frequency domain representations of uncompensated responses (top row), ICA-compensated responses (middle row) and the CI artifact determined with ICA (bottom row). Pulse periods are indicated in the time domain representation with vertical dotted lines. AM pulse trains presented in monopolar mode, between $0$ and $160$cu, $f_{\text{mod}} = 44$ Hz, $f_{\text{pulse}} = 900$ Hz, phase width $40$ µs, phase gap $8$ µs.

## 2.4. Experimental setup and signal processing

### *2.4.1. Subject*

Because infants cannot give reliable behavioural feedback, pilot data was obtained from one CI adult subject (age 57) implanted in the right ear. Her behavioural T- and C-levels were $105$ and $160$ current units (cu), determined based on $900$ pps biphasic symmetric pulse trains in monopolar mode presented between internal stimulation electrode $13$ and two external stimulation electrodes (MP1+2).

### *2.4.2. Stimuli*

The stimuli were generated electrically and sent to a programming device (POD) connected to an L34 research speech processor. Monopolar stimuli of approximately $5$ minutes were presented at stimulation electrode $13$, at a pulse rate of $900$ pps and amplitude modulated at $35$ and $44$ Hz.

### *2.4.3. Recording setup*

A $64$-channel Biosemi ActiveTwo EEG recording system based on a DC amplifier with $24$ bit resolution over a dynamic range of $524$ $\text{mV}_{\text{PP}}$ and a sampling rate of $8192$ Hz was used. The EEG signals were preamplified at the recording electrodes placed on the subject's head according to the positions of the international $10-20$ system. A trigger signal was sent to the recording system for synchronization.

### *2.4.4. Signal processing*

The EEG signal was high-pass filtered with a cut-off frequency of $2$ Hz and split into epochs of $2796$ samples ($0.34$ $s$), resulting in a frequency resolution of $3$ Hz. The CI artifact was either reduced using (1) blanking or (2) ICA. The ICs were computed using the Infomax algorithm as implemented in EEGLAB [16] applied to non-averaged data as suggested in [17]. ICs with spectral pulse rate amplitudes that contribute $5\%$ of the resulting epochs were rejected based on their peak to peak amplitudes to compensate for excessive motion and other artifacts; $848$ epochs (i. e., almost $5$ minutes) were used for the analysis. One-sample and two-sample Hotelling $\text{T}^2$ tests were applied to the signals recorded between recording

electrodes $P_6$, $P_8$, $P_{10}$, $TP_8$, $CP_6$, $PO_4$, $PO_8$ and reference electrode $C_z$. Electrophysiological thresholds were determined based on sigmoid functions fitted to the percentage of significant recording electrodes per stimulus intensity. The threshold was determined as the intensity at the intersection between the horizontal axis and the tangent to the sigmoid curve at the $50\%$ point.

## 3. RESULTS AND DISCUSSION

The analysis results for monopolar stimulation mode are shown in figure 3. For different artifact rejection techniques - (1) blanking and (2) ICA based CI artifact rejection - the amplitude growth and phase delay values are shown, as well as the results from the one- and two-sample tests. To increase statistical power, multiple recording electrodes (ME) and measurements at multiple recording electrodes and multiple stimulus intensities (ME+MI) were combined.

In the first and second row, response amplitude and phase delay for two modulation frequencies are shown in solid lines (ME) and in dashed lines (ME+MI). Response amplitudes ideally grow monotonously with increasing intensity and phase delay values should be constant for each modulation frequency. Phase delay values close to 180 degrees correspond to the phase delay of the CI artifact alone. The apparent latency of the response can be determined from the phase delay difference between the two modulation frequencies. For modulation frequencies in the $40$ Hz range, apparent latencies of about $50$ ms are expected.

In the third and fourth row, the p-values (pval) resulting from the statistical tests (significance level $5\%$) and percentage of significant recording electrodes ($\#$resp) are shown in solid and dashed lines, respectively.

The success of the artifact rejection techniques is difficult to assess as there is no artifact-free data available. However, small apparent latencies ($\ll 50$ ms) indicate that the artifact has not completely been removed. Furthermore, as the two-sample Hotelling $T^2$ test is not influenced by residual artifacts, it can serve as 'standard'.

With CI artifact rejection based on blanking, response amplitudes decrease slowly with decreasing intensity. The phase delay is dominated by the CI artifact, with a phase delay difference between the two modulation frequencies of about 90 degrees for stimulus intensities equal to or above $151$ cu. Results from the one-sample Hotelling $T^2$ test are inconsistent, with detected responses even at lower stimulus intensities. For the two-sample Hotelling $T^2$ test, response detection is reliable and responses are only detected at $151$ and $160$ cu. The electrophysiological threshold determined from the fitted sigmoid function based on the results of the two-sample test is $146.7$ cu.

In the case of ICA based CI artifact rejection, response amplitudes drop fast. At $151$ and $160$ cu, response amplitudes of about $100$ to $200$ nV are observed. For the lower stimulus intensities, response amplitudes are similar to the noise level of about $50$ nV. Whenever a significant response is seen, a phase delay difference between the two different modulation frequencies of about 180 degrees is observed, corresponding to an apparent response latency (group delay) of $55$ ms. This value is consistent with data for acoustical stimulation at modulation frequencies around $40$ Hz, with sources for these responses most probably located in the auditory cortex [7]. Both the one-sample and the two-sample Hotelling $T^2$ tests are able to reliably detect responses only at $151$ and $160$ cu. For the one-sample test, electrophysiological thresholds are $146.7$ cu and $150.8$ cu for $44$ Hz and $35$ Hz, respectively. For the two-sample test, the electrophysiological threshold is $146.7$ cu. The determined electrophysiological threshold of $146.7$ cu is located at about $70$ % of the dynamic range of the subject, which is similar to what can be found for stimulation in bipolar mode [5].

## 4. CONCLUSION

In this paper, an automatic EASSR CI artifact rejection technique based on ICA has been presented that is stable even in the presence of monopolar stimulation artifacts, and should allow the evaluation of response properties for clinically used stimuli. When compared to established methods for the response detection in the presence of stimulation artifacts, electrophysiological thresholds were similar while only requiring recordings for one modulation frequency. Furthermore, ICA based CI artifact rejection results in more reliable response amplitudes and phase latencies than blanking. ICA based CI artifact rejection can be developed further by replacing the simple thresholding method by more advanced techniques that take spatial information into account. More subjects should be tested, to check whether ICA manages to separate the CI artifact from the brain noise and EASSR response in all subjects and whether the determined threshold value can be generalized to other subjects.

## REFERENCES


[1] T. Boons, J.P.L. Brokx, I. Dhooge, J.H.M. Frijns, L. Peeraer, A. Vermeulen, J. Wouters, and A. van Wieringen, "Predictors of spoken language development following pediatric cochlear implantation.," *Ear Hear*, vol. 33, no. 5, pp. 617–39.

[2] N. Dillier, W.K. Lai, E. von Wallenberg, B. van Dijk, F. Akdas, M. Aksit, C. Batman, A. Beynon, S. Burdo, J.M. Chanal, and Others, "Normative findings of electrically evoked compound action potential measurements using the neural response telemetry of the Nucleus CI24M cochlear implant system," *Audiol Neurootol*, vol. 10, no. 2, pp. 105–116, 2005.

[3] C.A. Miller, N. Hu, F. Zhang, B.K. Robinson, and P.J. Abbas, "Changes across time in the temporal responses

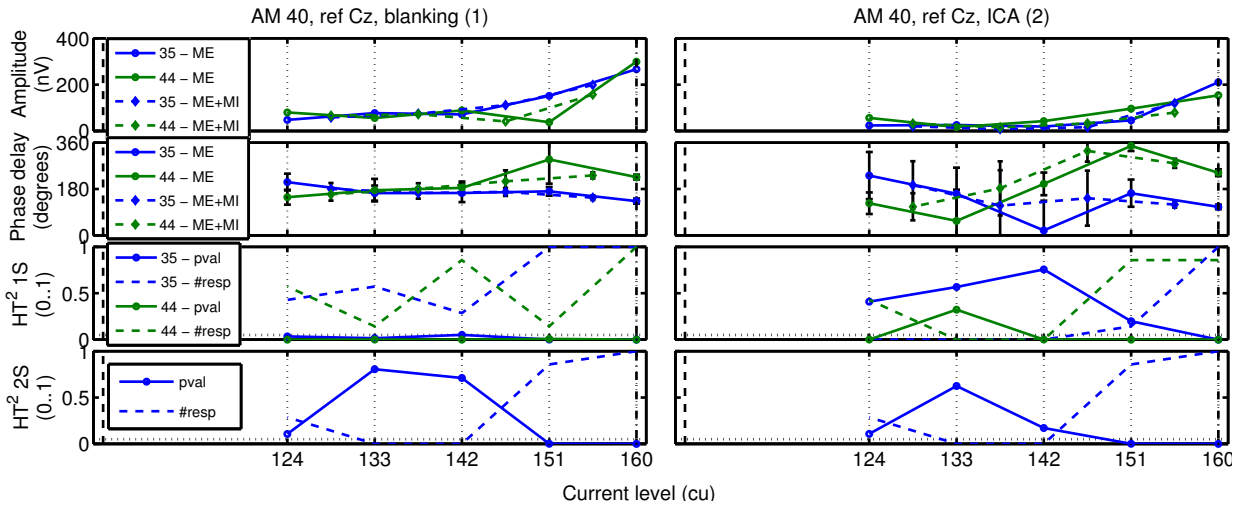


**Fig. 3**. EASSR response properties for AM pulse trains presented in monopolar mode at 900 pps with modulation frequencies 35 and 42 Hz. Stimulation electrode 13 and recording electrodes $P_8$, $P_{10}$, $TP_8$, $I_z$, $O_z$, reference recording electrode $C_z$. Left column: blanking (1), right column: ICA-based CI artifact rejection (2). First row: amplitude growth, second row: phase delay, third row: results of the one-sample Hotelling $T^2$ test, fourth row: results of the two-sample Hotelling $T^2$ test. Behavioural T- and C-levels are indicated with vertical dashed and dash-dot lines.


of auditory nerve fibers stimulated by electric pulse trains," *JARO*, vol. 9, no. 1, pp. 122–137, 2008.

[4] M. Hofmann and J. Wouters, "Electrically evoked auditory steady state responses in cochlear implant users," *JARO*, vol. 11, no. 2, pp. 267–282, 2010.

[5] M. Hofmann and J. Wouters, "Improved Electrically Evoked Auditory Steady-State Response Thresholds in Humans," *JARO*, vol. 13, no. 4, pp. 573–589, 2012.

[6] F.C. Jeng, P.J. Abbas, C.J. Brown, C.A. Miller, K.V. Nourski, and B.K. Robinson, "Electrically evoked auditory steady-state responses in Guinea pigs.," *Audiol Neurootol*, vol. 12, no. 2, pp. 101–112, 2007.

[7] T.W. Picton, M.S. John, A. Dimitrijevic, and D.W. Purcell, "Human auditory steady-state responses.," *Int J Audiol*, vol. 42, no. 4, pp. 177–219, June 2003.

[8] R.A. Dobie and M.J. Wilson, "A comparison of t test, F test, and coherence methods of detecting steady-state auditory-evoked potentials, distortion-product otoacoustic emissions, or other sinusoids.," *JASA*, vol. 100, pp. 2236–2246, 1996.

[9] B. Wilson and Z. Ghassemlooy, "Pulse time modulation techniques for optical communications: a review," *IEE Proc J Optoelectron*, vol. 140, no. 6, pp. 346, 1993.

[10] B.A. Martin, "Can the acoustic change complex be recorded in an individual with a cochlear implant? Separating neural responses from cochlear implant artifact.," *J Am Acad Audiol*, vol. 18, no. 2, pp. 126–140, 2007.

[11] P.M. Gilley, A. Sharma, M. Dorman, C.C. Finley, A.S. Panch, and K. Martin, "Minimization of cochlear implant stimulus artifact in cortical auditory evoked potentials.," *Clin Neuophysiol*, vol. 117, no. 8, pp. 1772–1782, Aug. 2006.

[12] L.M. Friesen and T.W. Picton, "A method for removing cochlear implant artifact.," *Hear res*, vol. 259, no. 1-2, pp. 95–106, Jan. 2010.

[13] D.E. Wong and K. Gordon, "Beamformer suppression of cochlear implant artifacts in an electroencephalography dataset.," *IEEE Trans Biomed Eng*, vol. 56, no. 12, pp. 2851–2857, Dec. 2009.

[14] F.C. Viola, J.D. Thorne, S. Bleeck, J. Eyles, and S. Debener, "Uncovering auditory evoked potentials from cochlear implant users with independent component analysis.," *Psychophysiology*, vol. 48, no. 11, pp. 1470–1480, Nov. 2011.

[15] F.C. Viola, M. De Vos, J. Hine, P. Sandmann, S. Bleeck, J. Eyles, and S. Debener, "Semi-automatic attenuation of cochlear implant artifacts for the evaluation of late auditory evoked potentials.," *Hear res*, vol. 284, no. 1-2, pp. 6–15, 2012.

[16] A. Delorme and S. Makeig, "EEGLAB: an open source toolbox for analysis of single-trial EEG dynamics including independent component analysis," *J Neurosci methods*, vol. 134, no. 1, pp. 9–21, 2004.

[17] S. Makeig, S. Debener, J. Onton, and A. Delorme, "Mining event-related brain dynamics.," *Trends Cogn Sci*, vol. 8, no. 5, pp. 204–10, May 2004.